5.1. McMurdo Station (01/24/06 – 1/12/07)

The 2006/07 season at McMurdo Station is defined as the period between the site visits 1/19/06 – 1/24/06 and 1/12/07 – 1/24/07. Season opening and closing calibrations were performed on 1/23/06 and 1/13/07, respectively. Volume 16 solar data comprise the period 01/24/06 – 1/12/07. A total of 16934 scans are part of the McMurdo Volume 16 dataset. There was virtually no loss of data due to technical problems. Variations in the monochromator's wavelength setting were larger than typical between September 2006 and January 2007. The wavelength uncertainty of data of this period is 0.05 nm ($\pm 1\sigma$).

A new building for the New Zealand Antarctic program was built at Arrival Heights during 2006 in approximately 20 meter distance from the U.S. facility. Construction involved the use of a drilling rig and other heavy equipment. Dust and shading from the activity may have affected solar measurements temporarily. Quality control of solar data did not indicate a significant impact from the construction.

5.1.1. Irradiance Calibration

The site irradiance standards for the McMurdo 2006/07 season were the lamps 200W005, 200W019, and M-543. Lamp 200W017 was used as traveling standard during both site visits. The lamp has been calibrated by Optronic Laboratories in March 2001. It was also compared with BSI's long-term standards (lamps 200W022 and M-763) on 6/1/06. At this time, the calibration of the three lamps agreed to within ±1.5%. Additional comparisons of lamp 200W017 with the San Diego site standard 200W028 performed during the second half of 2006 confirmed that the calibration of lamp 200W017 did not drift in 2006, and is consistent with the calibration of the San Diego standard.

The McMurdo site standard 200W019 has an Optronic Laboratories certificate from September 1998. The standard 200W005 was originally calibrated by Optronic Laboratories in November 1996. It has been recalibrated recently by comparison with standard 200W017, using scans performed during the 2006 site visit (see Volume 15 Operations Report). Lamp M-543 was lastly recalibrated in 2002 by comparison with the former traveling standard M-764, using scans performed during the site visits in 2001 and 2002.

Figure 5.1.1 shows the Volume 16 season opening calibrations, performed on 1/23/06. All site standards agreed at the ±1.5% level with the traveling standard 200W017. Figure 5.1.2 shows a similar plot based on the Volume 16 closing calibrations, performed on 1/13/07. The agreement is similar, but the pattern is different. For example, scans of lamp 200W019 were low by 1.5% relative to 200W017 on 1/23/05, but were high by approximately 1% on 1/13/07. The three site standards were also compared with each other on two additional days, namely 4/21/06 and 8/10/06. Results were consistent to within ±1% on both occasions. We note that discrepancies in the range of ±1.5% are still within the uncertainty of calibrations issued by standards laboratories.

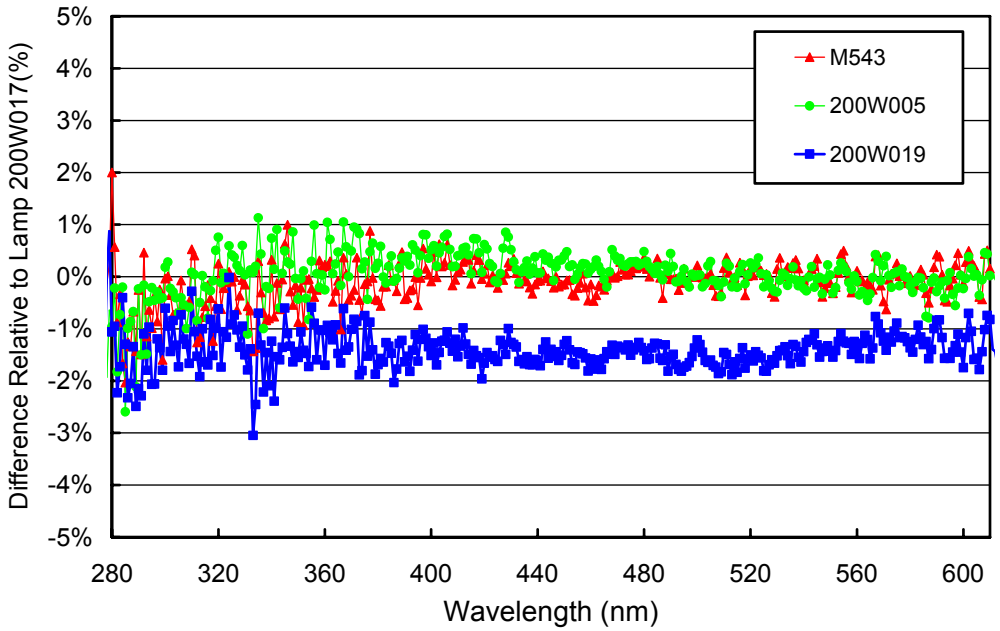

Figure 5.1.1. *Comparison of McMurdo lamps M-543, 200W005, and 200W019 with the BSI traveling standard 200W017 at the beginning of the season (1/23/06).*

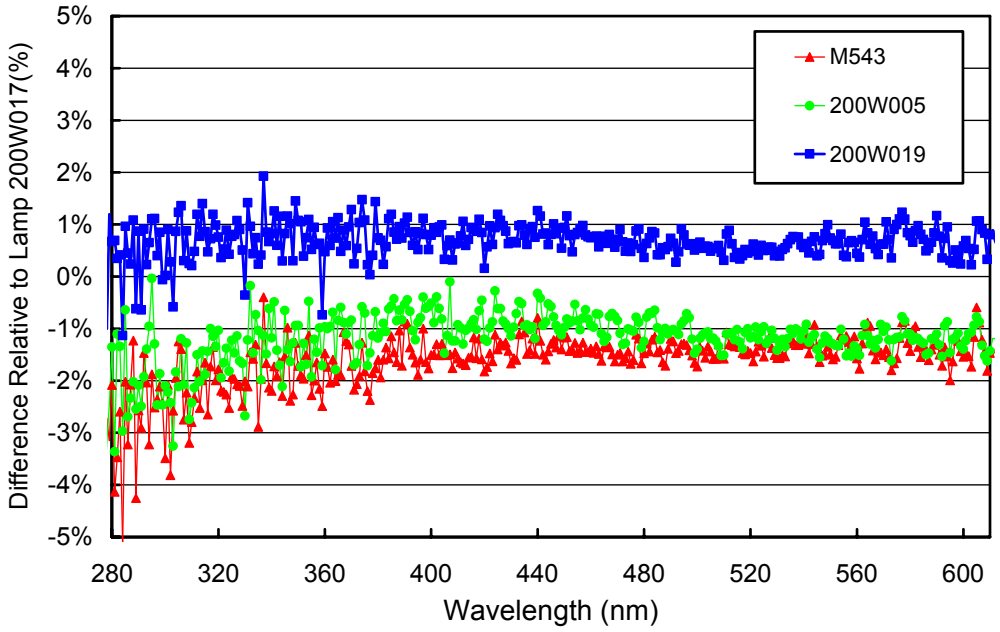

Figure 5.1.2. *Comparison of McMurdo lamps M-543, 200W005, and 200W019 with the BSI traveling standard 200W017 at the end of the season (1/13/07).*

5.1.2. Instrument Stability

The stability of the spectroradiometer over time is primarily monitored with bi-weekly calibrations utilizing the site irradiance standards and daily response scans of the internal irradiance reference lamp. The stability of this lamp is monitored with the TSI sensor, which is independent from possible monochromator and PMT drifts. By logging the PMT currents at several wavelengths during response scans, changes in monochromator throughput and PMT sensitivity can be detected.

Figure 5.1.3 shows changes in TSI readings and PMT currents at 300 and 400 nm, derived from the daily response scans. TSI measurements indicate that the internal reference lamp became brighter by approximately 2% over the course of the season. The PMT currents at 300 and 400 nm varied by ±2%, with lowest values in winter. This temporal pattern has been observed also in previous seasons and is probably related to seasonal changes in enclosure temperature. The actual reason is unknown. Changes in system response indicated in Figure 5.1.3 are automatically corrected during processing of solar data.

A total of four different calibrations were applied to the solar measurements of Volume 16. Figure 5.1.4 shows ratios of the calibration functions applied during Periods P2 - P4, relative to the function of Period P1. Changes from one period to the next are typically smaller than 1.5%. The calibration of period P1 was applied from January until the start of winter darkness. The calibration for Period P3 is based on two absolute scans only, and data were smoothed to reduce noise.

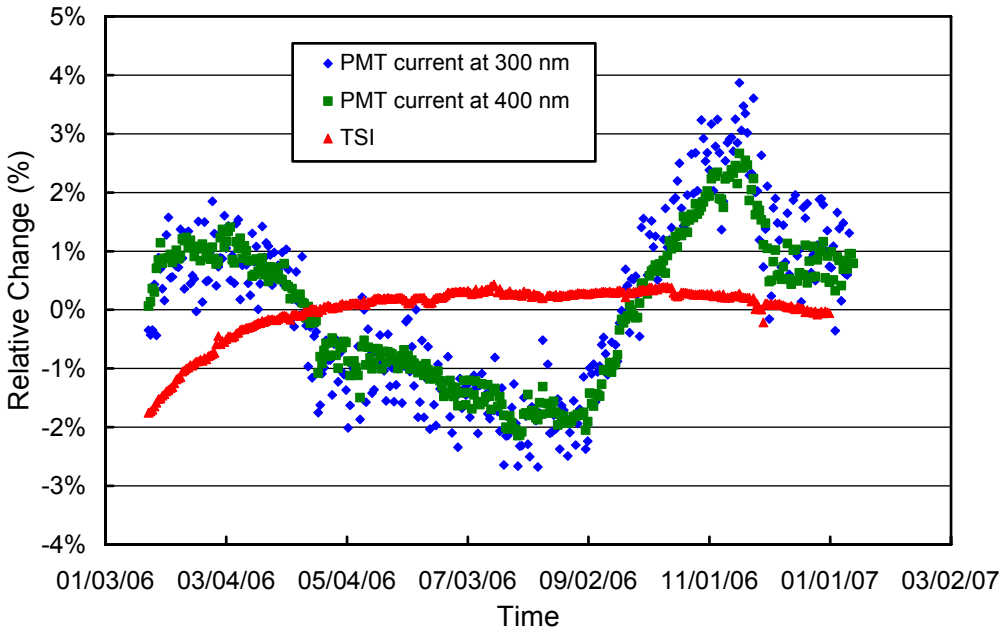

Figure 5.1.3. *Time-series of PMT current at 300 and 400 nm, and TSI signal derived from measurements of the internal irradiance reference lamp during the McMurdo 2006/07 season. Data are normalized to the average value of the whole season.*

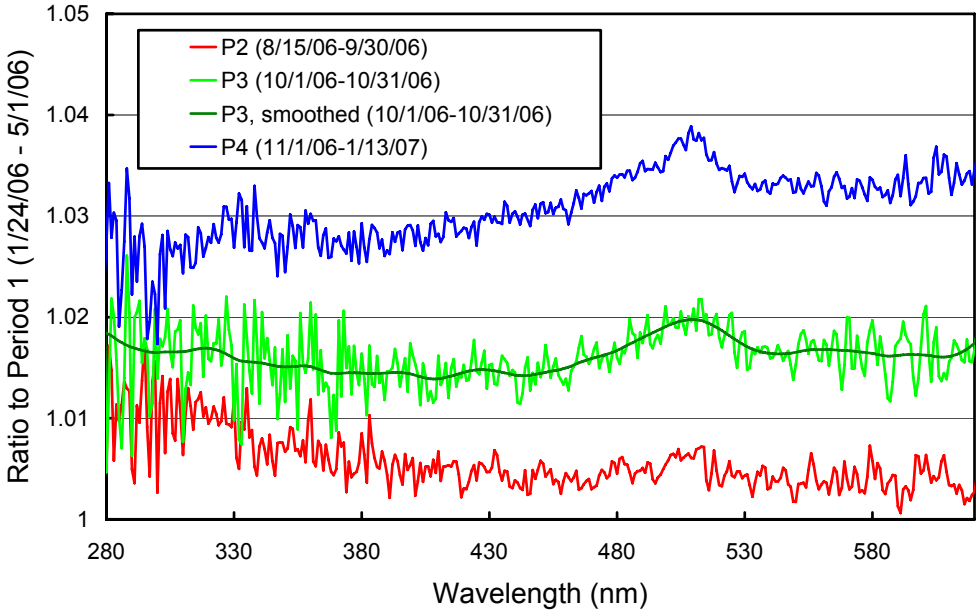

Figure 5.1.4 *Ratios of irradiance assigned to the internal reference lamp during periods P2 - P4, relative to Period P1.*

Figure 5.1.5 presents the relative standard deviation calculated from the individual absolute scans of each period. These data are useful for estimating the variability of calibrations performed in each period. The variability is typically less than 1.5% for wavelengths above 300 nm in all periods, indicating good consistency of individual absolute scans. Data of period P3 are noisy because the standard deviation was calculated from two absolute scans only. Solar data are not affected since a smoothed calibration function was used for processing solar measurements.

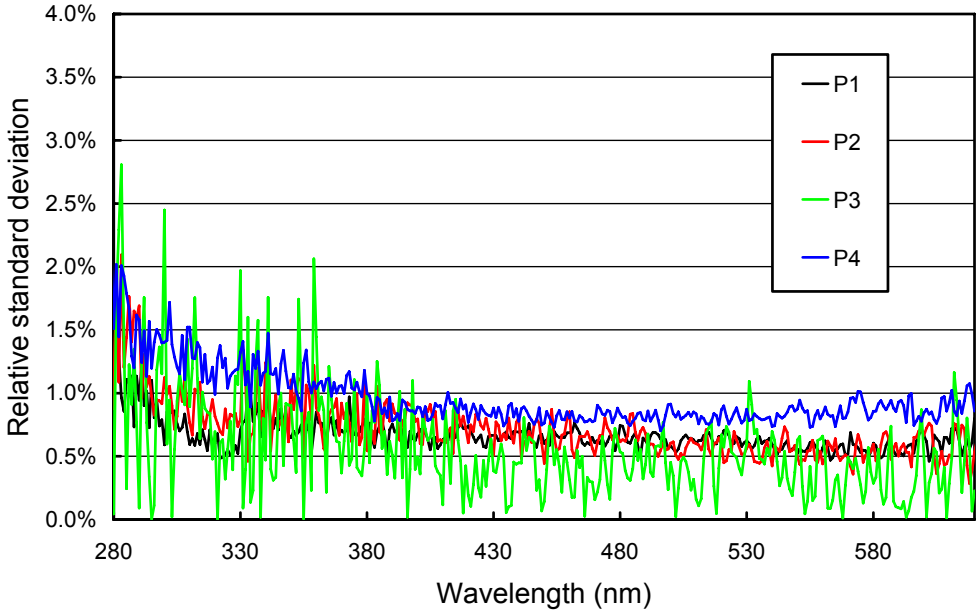

Figure 5.1.5. *Ratio of standard deviation and average calculated from absolute calibration scans performed in Periods P1 - P4.*

5.1.3. Wavelength Calibration

Wavelength stability of the system was monitored with the internal mercury lamp. Information from the daily wavelength scans was used to homogenize the data set by correcting day-to-day fluctuations in the wavelength offset. Figure 5.1.6 shows differences in the wavelength offset of the 296.73 nm mercury line between two consecutive wavelength scans. In total, 402 pairs of scans were evaluated. For 87% of the pairs, the offset change was smaller than ±0.025 nm; for 97% of the pairs it was smaller than ±0.055 nm. The wavelength difference between two consecutive scans was larger than 0.1 nm on three occasions, partly due to operator intervention. Data from these days were adjusted accordingly.

The wavelength stability was considerably better during the first part of the season (1/24/06 - 9/15/06; blue columns in Figure 5.1.6.) than during the second part (9/16/06 - 1/12/07; green column). Variations in the wavelength correction within one day are usually not corrected, and solar data from 9/16/06 onward have increased wavelength uncertainty. Inspection of the monochromator during the site visit in 2007 suggested that a worn bearing was the cause of the problem. The bearing was lubricated.

After data were corrected for day-to-day wavelength fluctuations, the wavelength-dependent bias between this homogenized data set and the correct wavelength scale was determined with the Version 2 Fraunhofer-line correlation method (Bernhard et al., 2004). This analysis confirmed the deterioration of the monochromator's wavelength stability after 9/16/06. In addition to increased variability, the monochromator's wavelength mapping started to oscillate with a periodicity of about one month. A large number of correction functions would have been necessary to correct for this periodicity. Handling of many functions is difficult to implement in the Version 0 processing routines, but can easily be addressed as part of processing of Version 2 data. We therefore decided to use three correction functions for Version 0 data only, and address corrections of the remaining fluctuations as part of processing of Version 2 data. Final Version 0 data from 9/16/06 onward have an increased wavelength uncertainty of about ±0.1 nm ($\pm 2\sigma$).

Figure 5.1.7 shows the three correction functions used for processing Version 0 data of the Volume 16 period. Figure 5.1.8 indicates the wavelength accuracy of final Version 0 data. Wavelength shifts were determined with the Version 2 Fraunhofer-line correlation method and are shown for five wavelengths in the UV and visible. Shifts from the first part of the year are typically smaller than ±0.05 nm. Shifts from the second part exhibit a periodicity of about one month, and typically vary between –0.1 nm and +0.1 nm.

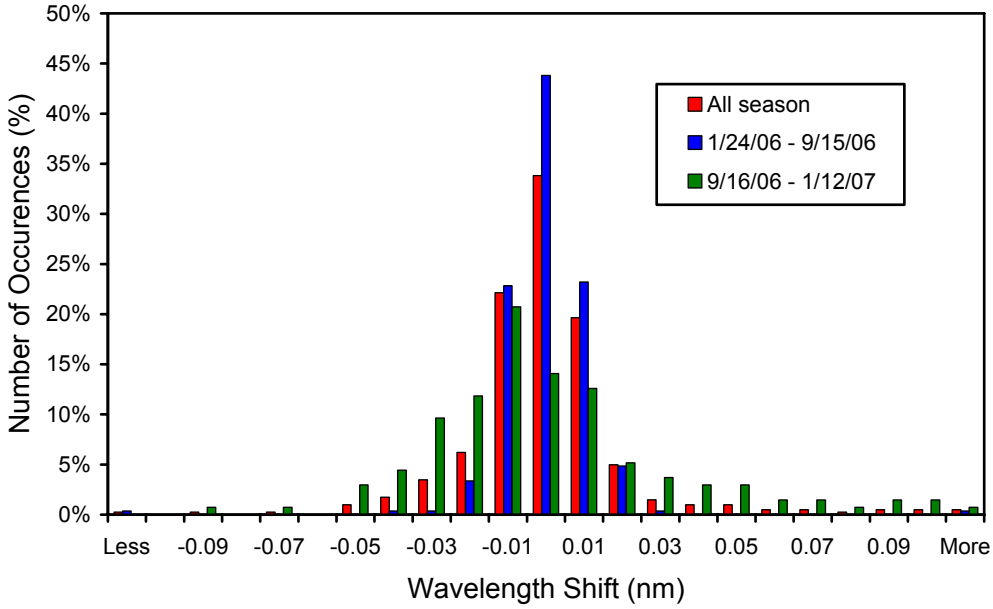

Figure 5.1.6. *Differences in the measured position of the 296.73 nm mercury line between consecutive wavelength scans. The x-labels give the center wavelength shift for each column. The 0-nm histogram column covers the range -0.005 to +0.005 nm. "Less" means shifts smaller than –0.105 nm; "more" means shifts larger than 0.105 nm.*

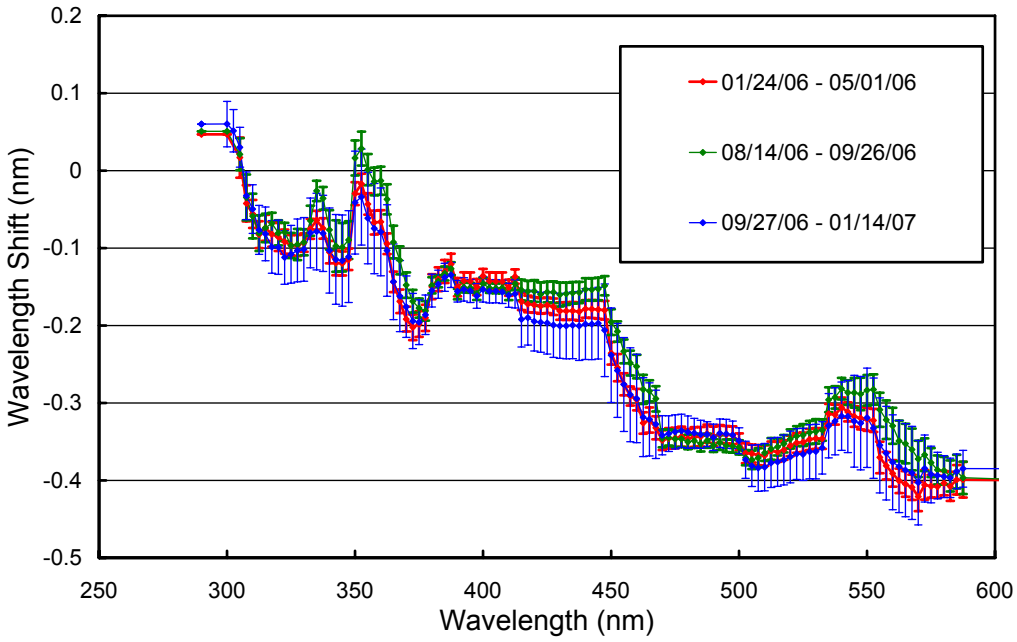

Figure 5.1.7. *Monochromator non-linearity correction functions for McMurdo 2006/07 data. Error bars indicate the 1σ-variation in each period.*

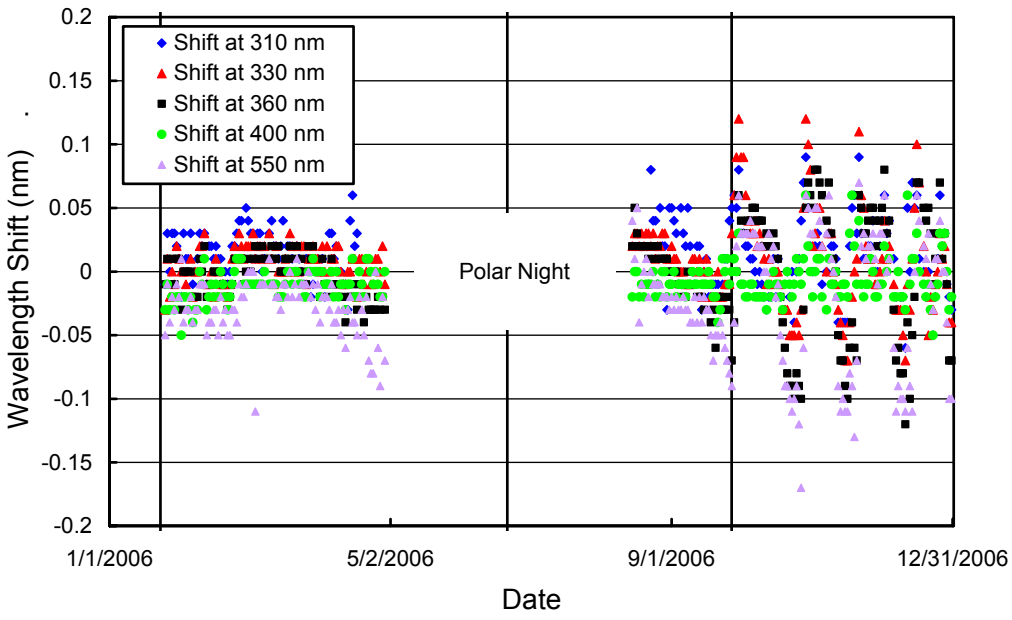

Figure 5.1.8. *Check of the wavelength accuracy of final data at four wavelengths by means of Fraunhofer correlation. The noontime measurement has been evaluated for each day of the season. No correlation data is available during Polar Night. Vertical lines indicate break points of non-linearity correction functions.*

Scans of the external mercury lamp do not have a direct influence on data products but are an important part of instrument characterization. Figure 5.1.9 illustrates the difference between internal and external mercury-lamp scans collected during the 2006 and 2007 site visits. The wavelength scale of the figure is the same as applied during solar measurements. The peak of the external scans agrees well with the nominal wavelength of 296.73 nm, whereas the peak of the internal scans is shifted by about 0.06 nm to shorter wavelengths. External scans have a bandwidth of about 1.02 nm FWHM. There is a small shift between the external scans from the 2006 and 2007 visits, which is caused by the increased wavelength uncertainty of measurements performed after September 2006. The bandwidth of the internal scan is 0.73 nm. External scans have the same light path as solar measurements and therefore represent the monochromator's bandpass at 297 nm that is relevant for solar scans.

5.1.4. Missing Data

A total of 16934 scans are part of the published McMurdo Volume 16 dataset. These are 96% of the maximum possible number of data scans. Of all missing data scans, 118, 293, and 290 were superseded by absolute, wavelength, and response scans, respectively. Only five scans were missed due to technical problems. Eleven additional scans were excluded from the published dataset because of shading of the instrument's collector, either by a nearby anemometer mast, personnel on the roof of the building, or construction of the new building for the New Zealand Antarctic program.

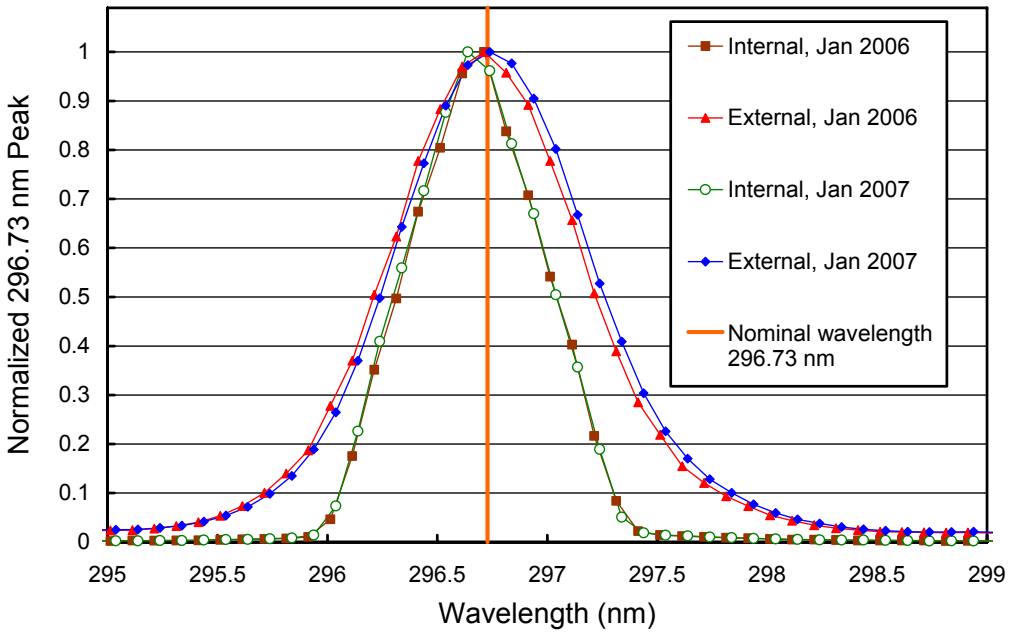

Figure 5.1.9 *The 296.73 mercury line as registered by the PMT from external and internal sources. The wavelength scale is the same as applied for solar measurements. It is assumed that the wavelength registration of the monochromator did not shift between internal and external scans, which were close in time.*

5.1.5. GUV Data

The GUV-511 radiometer, which is installed next to the SUV-100, was calibrated against final SUV-100 measurements following the method outlined in Section 4.3.1.

Data products were calculated from the calibrated measurements according to the procedure outlined in Section 4.3.2. Figure 5.1.10. shows a comparison of GUV-511 and SUV-100 erythemal irradiance based on final Volume 16 data. For solar zenith angles smaller than 80°, measurements of the two instruments agree to within ±2.7% (±1σ). Data from the GUV-511 radiometer tend to be low for large SZAs. We advise data users to use SUV-100 rather than GUV-511 data when the Sun is low.

Figure 5.1.11 shows a comparison of total ozone measurements from the GUV-511 radiometer and the Ozone Monitoring Instrument (OMI) installed on NASA's AURA satellite. GUV-511 ozone values were calculated as described in Section 4.3.3 and are plotted for SZAs smaller than 80°. On average, GUV-511 ozone values are larger by 3.2% than OMI data. The bias is larger for small ozone columns. This offset is partly caused by the influence of the ozone profile on calculations of the total ozone column, which has not been considered in the calculation of GUV-511 total ozone data. For most accurate total ozone information, we advise data users to use total ozone values calculated from SUV-100 measurements. These data are part of the "Version 2" dataset, available at www.biospherical.com/nsf/Version2/Version2.asp.

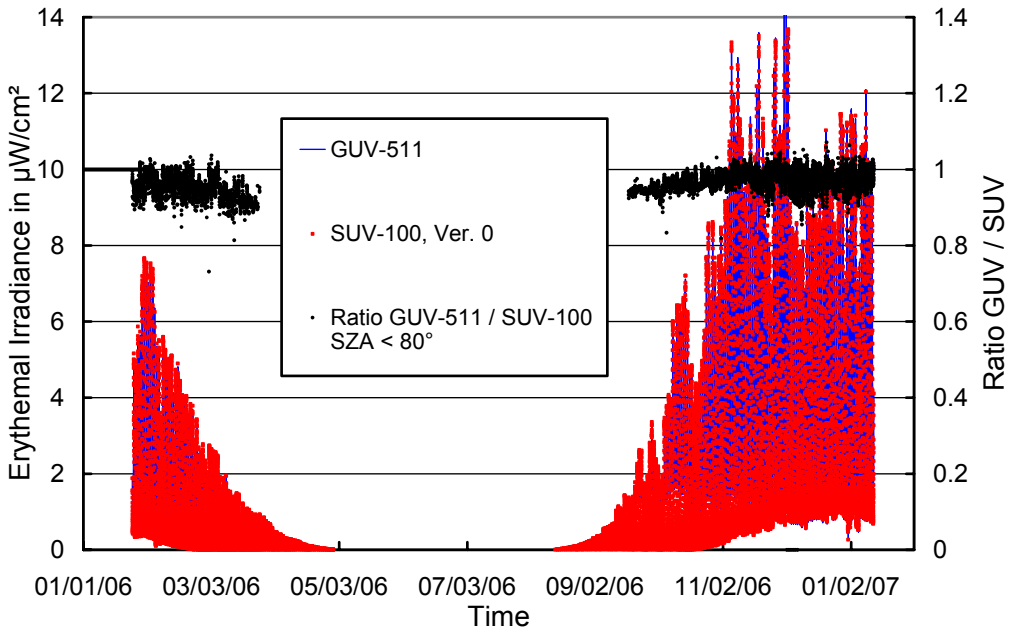

Figure 5.1.10. *Comparison of erythemal irradiance measured by the SUV-100 spectroradiometer and the GUV-511 radiometer. All data are based on "Version 0" (cosine-error uncorrected) data.*

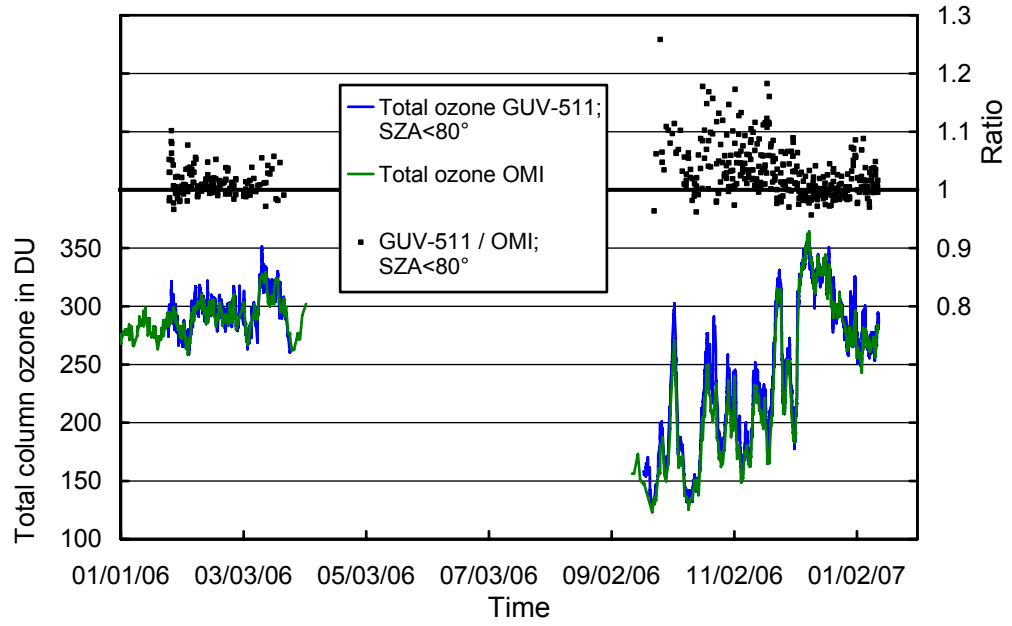

Figure 5.1.11. *Comparison of total column ozone measurements from GUV-511 and OMI. GUV-511 measurements are plotted in 15 minute intervals. For calculating the ratio of both data sets, only GUV-511 measurements concurrent with OMI overpass data were evaluated.*